Article

Analysis of Spectrum Sensing over Imperfect Channel conditions in Cognitive Vehicular Networks

Xiaomin Qian [1] iD **, Li Hao** [1,*]**, Dadong Ni** [1] **and Quang Thanh Tran**[1,2]

[1]   Key Lab of Information Coding and Transmission, Southwest Jiaotong University, Chengdu 610031, China; qxflying2009@163.com; lhao@swjtu.edu.cn; dadongni@hotmail.com
[2]   Faculty of Electrical and Electronic Engineering, University of Transport and Communications, Hanoi, Vietnam; thanhktvt@gmail.com
*   Correspondence: qxflying2009@163.com; Tel.: +86-180-3966-2390

Abstract: An explosive growth in vehicular wireless services and applications gives rise to spectrum resource starvation. Cognitive radio has been used to vehicular networks to mitigate the impending spectrum starvation problem by allowing vehicles to fully exploit spectrum opportunities unoccupied by licensed users. Efficient and effective detection of licensed user is a critical issue to realize cognitive radio applications. However, spectrum sensing in vehicular environments is a very challenging task due to vehicles mobility. For instance, vehicle mobility has a large effect on the wireless channel, thereby impacting the detection performance of spectrum sensing. Thus, gargantuan efforts have been made in order to analyze the fading properties of mobile radio channel in vehicular environments. Indeed, numerous studies have demonstrated that the wireless channel in vehicular environments can be characterized by a temporally correlated Rayleigh fading. In this paper, we focus on energy detection for spectrum sensing and a counting rule for cooperative sensing based on Neyman-Pearson criteria. Further, we go into the effect of the sensing and reporting channels condition on spectrum sensing performance under temporally correlated Rayleigh sensing channel. For local and cooperative sensing, we derive some alternative expressions for average probability of miss detection. The pertinent numerical and simulating results are provided to further validate our theoretical analyses under a variety of scenarios.

Keywords: Cognitive radio, Cognitive vehicular networks, Spectrum sensing, Sensing/Reporting channel, Correlated Rayleigh fading channel, Hard fusion.

1. Introduction

Vehicular networks serve as an actual enabling application that is conceived to enhance road safety and provide in-vehicle infotainment for passengers on the road by allowing vehicle-to-vehicle (V2V) as well as vehicle-to-infrastructure (V2I) communications. It has attracted substantial investigation from industries and research institutions in the last few years and still faces a host of challenges before starting the actual implementation. One major challenge is the deficient frequency resources available for wireless communications in vehicular networks.

Currently, the Federal Communication Commission (FCC) has reserved 75-MHz licensed spectrum bandwidth (i.e., seven 10-MHz channels) at a center frequency of 5.9-GHz in support of dedicated short-range communication (DSRC) in vehicular environments. However, a tremendous increase in wireless applications being developed for vehicular communications, may give rise to serious congestion of the band, and ultimately reducing the communication efficient for safety applications. Moreover, not only road safety applications, but also the increasing number of

32　applications related to infotainment systems will also lead to channel contention and spectrum
33　deficiency. In view of the stringent QoS requirements on DSRC spectrum, it is not be sufficient
34　for all applications to depend only on the 5.9-GHz DSRC spectrum. There is a dramatic increase in the
35　demand for frequency resources to satisfy their communication requirements.

36　　　To relieve the bottleneck problem of spectrum deficiency, cognitive radio (CR) [1], [2] has
37　increasingly been presented as a potential technique being capable of accessing licensed but unoccupied
38　frequency bands only without causing any unacceptable interference to licensed users (or primary
39　users, PUs). Cognitive radio has become one of the most breathtaking technologies to improve the
40　spectrum efficiency effectively for the past couple of decades. In addition to a better remedy for
41　frequency scarcity issue, cognitive radio is appropriate for vehicular environments, since their unique
42　characteristics make it much better to achieve the spatial and temporal reusage of the empty frequency
43　bands of PUs compared to other traditional cognitive networks [3], [4]. To efficiently reutilize the
44　spectrum holes with minimum interference to PUs, the CR-enabled vehicles, which can be called
45　secondary vehicular users (SVUs), need to reliably make a decision about the existence of PUs. And
46　they must immediately vacate the radio channels as soon as PUs are detected. Consequently, spectrum
47　sensing constitutes the key component of cognitive vehicular networks (CVNs) [7].

48　　　Spectrum sensing [5] is a wealthily investigated subject, but is more concentrated in traditional
49　CR networks. Among them, cooperative sensing [6] has already attracted strong research interest as it
50　can take further advantage of both spatial and temporal diversity, and thereby garner better sensing
51　accuracy and efficiency in the face of fading. However, these existing spectrum sensing techniques can
52　not be directly applicable to vehicular networks. And it's all because we have to give an account of the
53　idiosyncrasies of vehicular networks such as high mobility while designing sensing schemes for CVNs
54　[3], [8]. For instance, rapid movement of vehicles makes the availability of spectrum holes dynamically
55　change since a vehicle may enter or leave a region interfered by a particular PU at different locations
56　along the road. In this regard, it is considerable for SVUs to detect PU activities in the fastest possible
57　way. Additionally, the vehicles' motion are restricted and predictable due to the fixed road topology.
58　In consequence, each vehicle may be glad to know in advance the spectrum opportunities to better
59　utilize them for transmission on its track. Further, high speeds and the environmental clutter can affect
60　the received signal due to Doppler effect, fading and shadowing. These factors will have immediate
61　impacts on spectrum sensing of CVNs.

62　　　Spectrum sensing in dynamic vehicular environments have been researched in some preliminary
63　works [4], [9], [10], [11], [12]. The authors in [4] proposed a novel adaptive sensing coordinated
64　mechanism, in which the central node merely assist and coordinate the SVUs to better acquire the
65　availability of spectrum holes instead of completely controlling the sensing and access. The authors
66　in [9] studied the detection performance of spectrum sensing under the shadowing and multi-path
67　composite fading channel in vehicular environments. The authors in [10] presented an asynchronous
68　collaborative sensing framework in which the tagged vehicle collects energy measurements labeled
69　with time and location information from collaborative SVUs and assigns weights based on their storing
70　time and location. The authors in [11] proposed a distributed collaborative sensing scheme based
71　on adaptive decision threshold for sensing and voting scheme for connected vehicles. An integrated
72　overview of spectrum sensing in cognitive vehicular environments can be discovered in [12]. None
73　of these previous researches considered the effect of temporal correlation due to vehicle motion and
74　multi-path propagation in a mobile vehicular environment. Moreover, the reporting channels between
75　SVUs and the fusion center (FC) were assumed to be ideal.

76　　　In this paper, our attention is centered on large-scale fixed PUs detection in an infrastructure-based
77　CVN based on mutual benefit and acquiring a win-win situation by allowing the back vehicles utilize
78　the spectrum availability information after front vehicles sensed. Each SVU periodically performs
79　sensing and reports its sensing information via the dedicated reporting channel to the nearby FC.
80　The FC fuses the received information to make a global decision for the current cell. At this moment,
81　some vehicles taking part in cooperative sensing may have left this cell. We investigate the sensing

performance using hard fusion [13]. Although soft fusion can gather improved performance than hard fusion, the burden of reporting overhead impedes its applicability [14]. Our research in this paper distinct from the previous works in two respects: 1) look at the effect of fading correlation and their severity on spectrum sensing performance under temporally correlated Rayleigh sensing channel; and 2) make clear how dramatically the reporting channel conditions could influence the reliability of a local/global decision, when made by the FC. For local and cooperative sensing, we evaluate the sensing performances through theoretical analysis or Monte Carlo simulation. Our results shows that poor channel conditions harms the detection performance. However, amazingly, we will demonstrate that the fast time-varying characteristic of sensing channels can give us an opportunity to obtain temporal diversity provided that a proper sensing technique is adopted.

The rest of the paper is organized as follows. In Section 2, we describe system model and assumptions on spectrum sensing in vehicular environments. In Section 3, the local sensing performance over correlated Rayleigh fading is analyzed. In Section 4, we consider the cooperative sensing performance with fading reporting channels. This is followed by the numerical and simulated results in Section 5. Lastly, we summarize the conclusions in Section 6.

Throughout this paper on detection performance, we will declare the local probabilities of false alarm, miss detection, and detection as P_f, P_m, and P_d, respectively, whereas their equivalent local probabilities will be represented by P_F, P_M, and P_D and their global probabilities Q_f, Q_m, and Q_d for hard fusion.

2. System Model and Problem Formulation

In this section, we briefly introduce the network model, the channel model, the sensing model, and the assumptions made in the CVNs under consideration.

2.1. Network Model

We consider a vehicular network in multi-lane highway scenarios in which licensed and cognitive users coexisting peacefully within the same geospatial region and share multiple frequency channels, like the one depicted in Fig.1. We suppose a large-scale fixed licensed user, such as licensed DTV spectrum holders. The cognitive network is an infrastructure-aided network, in which each cell is composed of a fusion center and a number of associated SVUs. The FC coordinates SVUs collaborative sensing and their access to a vacant PU channel. Each SVU periodically performs sensing and reports its sensing information via the dedicated reporting channel to the nearby FC. According to the received local sensing results, the FC arrives at a global decision for the current cell. At this moment, some vehicles engaged in cooperative sensing may have left this cell. Hence, the FC diffuses the global decision to the next passing SVUs. We postulate that the vehicles move independently from any other, and thus, the sensing channels between PU and SVUs are all independent of one another.
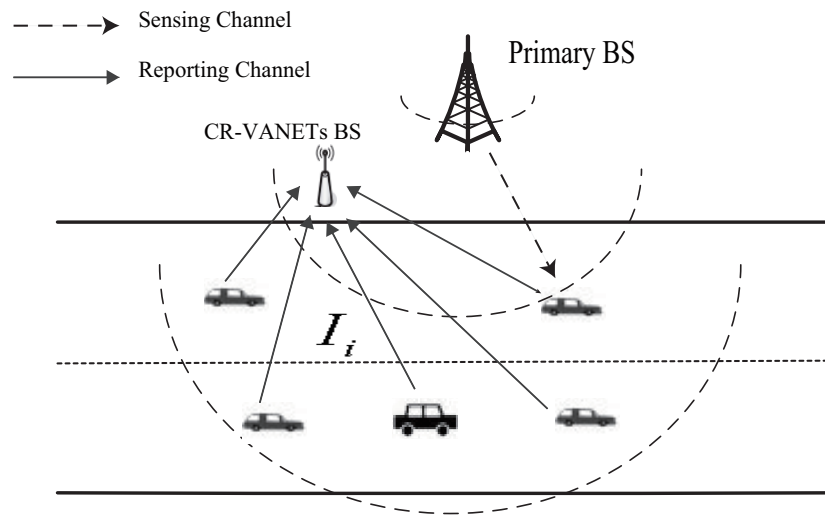
Figure 1. An illustrative example of cooperative sensing operation for cognitive vehicular networks. There are a PU, cooperative SVUs, and a CR-BS over wireless sensing/reporting channels.

2.2. Channel Model

In the above scenario, we consider the wireless channels, which have no correlation in space but are temporally correlated following the Jakes' model of land mobile fading channel (Table 2.1 in [15]). Let $\rho(\tau)$ denotes the correlation coefficient between two samples separating τ time interval, which satisfies

$$\rho(\tau) = \mathcal{J}_0(2\pi F_d T_s \tau) \tag{1}$$

where $\mathcal{J}_v(\cdot)$ is defined by the vth-order Bessel function of the first kind, and $F_d T_s$ represents normalized Doppler shift, $F_d T_s = \frac{f_c v}{c} T_s$, which may relate to a vehicle speed v, a carrier frequency f_c and the sampling interval T_s.

The correlation specialities of the fading progress depend only on $F_d T_s$, as illustrated in fig. 2. Based on the different $F_d T_s$, we can employ a suitable model, which is convenient to analyze the fading characteristics of sensing channel. For instance, three different models, $\mathcal{M}_1$, $\mathcal{M}_2$ and $\mathcal{M}_3$, are given as follows, respectively

$\mathcal{M}_1$: When $F_d T_s$ is relatively smaller (< 0.001), the channel process is nearly time-invariant.

$\mathcal{M}_2$: When $F_d T_s$ is small (< 0.02), the channel process is correlated ("slow" fading).

$\mathcal{M}_3$: For larger values of $F_d T_s$ (> 0.03), the channel process are almost independent time-varying ("fast" fading).

Note that $\mathcal{M}_1$ and $\mathcal{M}_3$ are two extreme cases of temporally correlated Rayleigh fading channel.
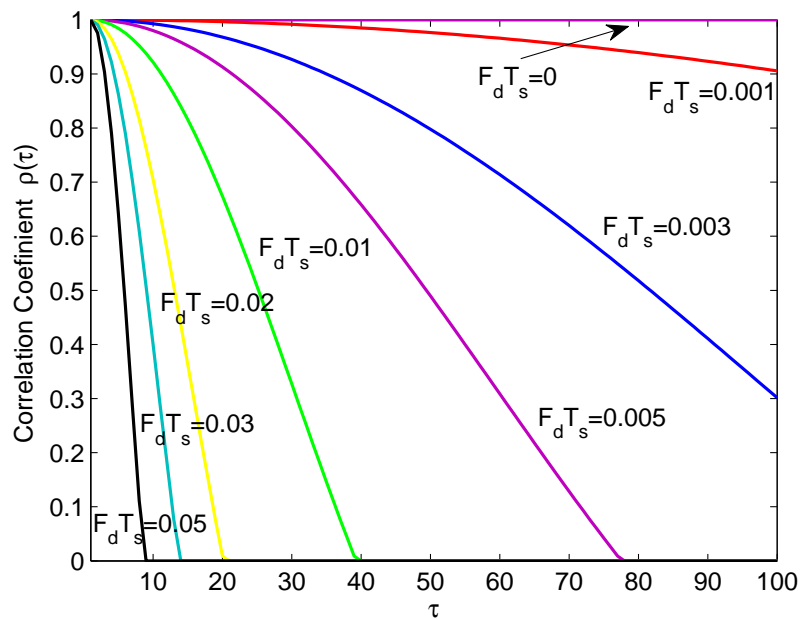
Figure 2. The correlation coefficient for various $F_d T_s$.

2.3. Sensing Model

Spectrum sensing is a binary hypothesis detection issue, with the null ($\mathcal{H}_0$) and alternative ($\mathcal{H}_0$) hypotheses associated to the presence and absence of PU in a given frequency band, respectively. We consider a cognitive vehicular network consisting of N collaborative SVUs. Assume L sampling observations can be used within a sensing interval. Under both hypotheses, the received observation by SUV i at the kth time instant can be expressed as, respectively

$$x_i(k) = \begin{cases} n_i(k) & \mathcal{H}_0 \\ h_i(k)s(k) + n_i(k) & \mathcal{H}_1 \end{cases} \tag{2}$$

where, $s(k)$ is the baseband-equivalent signal transmitted by the PU, $x_i(k)$ denotes the received signal by SVU i, $h_i(k)$ denotes the sensing channel gain with $E[|h_i(k)|^2] = 1$, and $n_i(k)$ denotes white and circularly symmetric complex Gaussian (CSCG) noise with mean zero and variance σ_n^2, i.e., $n_i(k) \sim \mathcal{CN}(0, \sigma_n^2)$. It's assumed that $s(k)$, $h_i(k)$ and $n_i(k)$ are independent of each other, which is reasonable from a practical situation.

To reduce the complexity and reporting channel overhead, each SVU employs a mapping rule to its observations, to produce a quantized information denoted by $q(x_i)$. In this paper, we suppose each SUV makes a binary decision $u_i = q(x_i) \in \{+1, -1\}$ with probabilities of false-alarm and mis-detection P_{fi} and P_{mi}. These decisions are then reported to the FC via a fading reporting channel or link, bit error may happen, which further affects the sensing performance at the FC. We will model the reporting channel as a Rayleigh fading channel. The received observation at the FC from the ith node can be descried as

$$z_i = g_i u_i + w_i \tag{3}$$

where g_i is the fading gain of reporting channel and w_i is a zero-mean Gaussian random variable with variance δ_i^2, i.e., $w_i \sim \mathcal{N}(0, \delta_i^2)$. Once the noisy observation $\{z_i; i = 1, 2, \cdots, N\}$ is received and decoded, the FC makes a global decision on which hypothesis is more likely to be true.

138   In the ordinary sense, an optimal fusion rule for hard combination is behaved in the form of
139   a counting rule [16]. This argument proves to be true even when those decisions are received via
140   unreliable communication channels, provided that the channels are also independent and identical
141   distribution (IID). In the latter of this paper, we focus on energy detection for spectrum sensing and
142   look at the detection performance of the counting rule in Rayleigh fading channels.

3. Local Sensing with Energy Detection

144   For local sensing, we consider energy detection (ED) instead of other sensing techniques, such as
145   the cyclostationary feature detection which takes high computational complexity and much longer
146   sensing time because it exploits a specific signature of the PU signal. Energy detection [17], [18] is
147   the most practical and robust detection method because it merely estimates the signal energy on
148   the considered band and produces very good performance without any *priori* information about PU
149   signals, as illustrated in fig. 3. Furthermore, Energy detection is a viable choice for vehicular networks
150   on account of its high mobile environment and low latency tolerant.
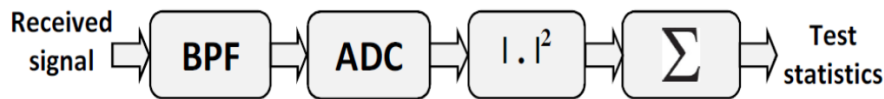

Figure 3. Energy detector model.

Consequently, the local test statistic of the energy detector at the ith SUV, denoted by e_i, is basically
an estimate of received signal energy which is represented as:

$$e_i = \sum_{k=0}^{L-1} |x_i(k)|^2 \qquad (4)$$

Let λ denotes the local decision threshold and u_i denote the local decision of the ith SVU, the
decision rule used by energy detector at each SVU can be expressed as

$$u_i = \begin{cases} +1 & if \quad e_i \geq \lambda \\ -1 & if \quad e_i < \lambda \end{cases} \qquad (5)$$

151   This means that when e_i is greater than or equal to λ, SVU i makes its individual decision u_i =+1
152   which tells PU signal is detected ($\mathcal{H}_1$); otherwise, it makes a decision u_i =-1 which declares that PU
153   signal is not detected ($\mathcal{H}_0$).

For a high number of sensing observations L, on the basis of the Central Limit Theorem (CLT),
the local test statistic e_i given by (3) can be well modeled by a normal or Gaussian distribution under
either $\mathcal{H}_0$ or $\mathcal{H}_1$ [17]. Accordingly, the probability density function (PDF) of e_i at individual SVU can
be compactly characterized by

$$e_i \sim \begin{cases} \mathcal{N}(L\sigma_n^2, L\sigma_n^4) & \mathcal{H}_0 \\ \mathcal{N}\left[(L+\eta_i)\sigma_n^2, (L+2\eta_i)\sigma_n^4\right] & \mathcal{H}_1 \end{cases} \qquad (6)$$

where

$$\eta_i = \sum_{k=0}^{L-1} |h_i(k)|^2 \frac{E_s}{L\sigma_n^2} \qquad (7)$$

154   represents the instantaneous signal-to-noise ratio (SNR) experienced by the i-th SVU within the current
155   sensing period. It is straightforward to see that η_i varies from (sensing) period to period, since it

generally hinges upon the fading characteristics of the wireless channel. And $E_s = \sum\limits_{k=0}^{L-1} |s(k)|^2$ denotes the transmitted signal energy by the primary user over a sensing interval of L sampling observations.

In the above discussed case, the probabilities of false alarm, miss detection and detection for local sensing at the i-th SVU can be represented by the following formulas, respectively

$$P_{fi}(\lambda) = P\left(e_i \geq \lambda | \mathcal{H}_0\right) = \mathcal{Q}\left(\frac{\lambda - L\sigma_n^2}{\sqrt{L}\sigma_n^2}\right) \tag{8}$$

$$P_{di}(\lambda) = P\left(e_i \geq \lambda | \mathcal{H}_1\right) = \mathcal{Q}\left(\frac{\lambda - (L + \eta_i)\sigma_n^2}{\sqrt{L + 2\eta_i}\sigma_n^2}\right) \tag{9}$$

$$P_{mi}(\lambda) = P\left(e_i < \lambda | \mathcal{H}_1\right) = \mathcal{Q}\left(\frac{(L + \eta_i)\sigma_n^2 - \lambda}{\sqrt{L + 2\eta_i}\sigma_n^2}\right) \tag{10}$$

where $\mathcal{Q}(x)$ is defined by the complementary cumulative distribution function of the standard Gaussian, i.e., $\mathcal{Q}(x) = \frac{1}{\sqrt{2\pi}}\int_x^\infty \exp(-\frac{t^2}{2})dt$.

It's apparent that, P_{fi} in (8) is independent of received SNR because P_{fi} is considered for the hypothesis of no PU signal transmission. On the other hand, P_{mi} in (10) is a conditional probability depending on instantaneous received SNR η_i. In this circumstance, the average P_m can be calculated by integrating the conditional P_{mi} over the SNR fading distribution [17], or quantify the quality of each channel by its corresponding average received SNR.

From (8) and (10), we also see that, λ can be analytically set to maintain the desired P_f if P_f is designated as the constraint of the detection problem. Then, we obtain P_{mi} related to the desired P_f as follows

$$P_{mi}(\eta_i) = \mathcal{Q}\left(\frac{\eta_i - \sqrt{L}\mathcal{Q}^{-1}(P_f)}{\sqrt{L + 2\eta_i}}\right) \tag{11}$$

where $\mathcal{Q}^{-1}(x)$ is defined by the inverse function of $\mathcal{Q}(x)$.

Next, we first consider the case of $\mathcal{M}_1$, in which the vehicles move more slowly, F_dT_s is small (< 0.001). And thus, the channel gain $h_i(k)$ remain virtually unchanged during the sensing interval, i.e., $h_i(k) = h_i$ for $k = 1, 2, \cdots, L$. Thus, η_i given by (7) can be rewritten as:

$$\eta_i = |h_i|^2 \frac{E_s}{\sigma_n^2} = |h_i|^2 \eta_s \tag{12}$$

where $\eta_s = \frac{E_s}{\sigma_n^2}$ is the local average SNR measured at the secondary receiver. It is thus note-worthy that the local average SNR is L times more than the average SNR measured at the energy detector output, which can be expressed as $\eta_0 = \frac{E_s}{L\sigma_n^2}$.

Under Rayleigh fading, the instantaneous SNR η_i can be viewed as exponentially distributed

$$f_{\eta_i}(\eta_i) = \frac{1}{\eta_s}e^{-\eta_i/\eta_s} \tag{13}$$

For ease of calculation, we make the following approximation for equation (11) as

$$P_{mi}(\eta_i) \approx \mathcal{Q}\left(\frac{\eta_i - \sqrt{L}\mathcal{Q}^{-1}(P_f)}{\sqrt{L + 2\eta_s}}\right) \tag{14}$$

In what follows we shall define, for the sake of conciseness

$$A = \frac{1}{\sqrt{L + 2\eta_s}}, B = \frac{\sqrt{L}\mathcal{Q}^{-1}(P_f)}{\sqrt{L + 2\eta_s}}$$

then

$$P_{mi}(\eta_i) \approx \mathcal{Q}\left(A\eta_i - B\right) \tag{15}$$

Consequently, the average P_m in the case of $\mathcal{M}_1$, $\overline{P}_m$, can be calculated by integrating (15) over (13) and making the change of variable $x = A\eta - B$ yielding

$$
\begin{aligned}
\overline{P}_m &= \int_0^\infty P_m(\eta_i) f_{\eta_i}(\eta_i) d\eta_i \\
&\approx \frac{1}{\eta_s} \int_0^\infty \mathcal{Q}\left(A\eta_i - B\right) e^{-\eta_i/\eta_s} d\eta_i \\
&= \frac{1}{A\eta_s} \int_{-B}^\infty \mathcal{Q}\left(x\right) e^{-\frac{x+B}{A\eta_s}} dx
\end{aligned}
\tag{16}
$$

By capitalizing on the integrating characters of $\mathcal{Q}$-function [19], and after some simplification, we can derive the following formula for $\overline{P}_m$

$$\overline{P}_m \approx \mathcal{Q}(-B) - e^{-\frac{B}{A\eta_s}} e^{\frac{1}{2A^2\eta_s^2}} \mathcal{Q}\left(\frac{1}{A\eta_s} - B\right) \tag{17}$$

In the case of $\mathcal{M}_2$, in order to obtain $\overline{P}_m$ in closed form, it desirable to obtain the PDF of η_i given in (7). Unfortunately, So far as is known, there is no closed-form expression available for such a distribution. Therefore, it is computationally infeasible to obtain a closed-form expression for $\overline{P}_m$ in the present of temporal fading correlation. Instead of deriving a closed-form for $\overline{P}_m$, we estimate $\overline{P}_m$ through a Monte Carlo simulation.

Highly mobility of vehicles lead to an increase in Doppler shift $F_d T_s$, and thereby resulting in degraded correlation among sampling observations. In the case of $\mathcal{M}_3$, the sampling observations of the fading channel $\{h_i(k)\}$ are completely independent of each other, η_i given by (7) can be reduced to the following equation

$$\eta_i = \frac{E_s}{\sigma_n^2} \tag{18}$$

It is plain to see that η_i is independent of instantaneous fading statistics. Thus, the $\overline{P}_m$ in this case can be computed directly by (10) and (18).

4. Cooperative Sensing with Counting Rule

The concept of cooperative spectrum sensing is to utilize multiple SVUs at different locations and fuse their independent sensing messages into one unified decision inferring the presence or absence of the PU. In this section, we will ponder this approach based on hard fusion, and also look at the impact of the reporting channel fading to the global detection performance.

4.1. Equivalent Local Probability of False Alarm and Miss Detection

In consideration of the unreliable characteristic of the reporting channels, let us determine its effect on the reliability of the decision made by the FC. Let v_i denote the decoded version of z_i for the ith SVU at the FC, the decoded rule can be expressed as

$$v_i = \begin{cases} 1 & if \quad z_i \geq 0 \\ 0 & if \quad z_i < 0 \end{cases} \tag{19}$$

And, more remarkable, under the hypothesis $\mathcal{H}_j$ $(j = 0, 1)$

$$
\begin{aligned}
\mathrm{E}[v_i \,|\, \mathcal{H}_j] &= P(v_i = 1 \,|\, \mathcal{H}_j) \times 1 + P(v_i = 0 \,|\, \mathcal{H}_j) \times 0 \\
&= P(z_i \geq 0 \,|\, \mathcal{H}_j)
\end{aligned}
\tag{20}
$$

$$
\begin{aligned}
\mathrm{D}[v_i \,|\, \mathcal{H}_j] &= \mathrm{E}[v_i^2 \,|\, \mathcal{H}_j] - \mathrm{E}[v_i \,|\, \mathcal{H}_j]^2 \\
&= P(z_i \geq 0 \,|\, \mathcal{H}_j) - \left(P(z_i \geq 0 \,|\, \mathcal{H}_j) \right)^2
\end{aligned}
\tag{21}
$$

where $\mathrm{E}[x]$, $\mathrm{D}[x]$ denotes the expectation and variance operator with respect to x.

As can be seen from (20) and (21), the expectation and variance of received decision v_i are directly depend on the probability $P(z_i \geq 0 \,|\, \mathcal{H}_j)$, which can also be referred to the equivalent probability of false-alarm and mis-detection of local sensing. For notational convenience, let us denote this probability by P_{Fi} and P_{Di} under both hypothesis. In order to capture the statistical properties of v_i, we first need to obtain the probabilities $P_{Fi} = f(z_i \geq 0 | \mathcal{H}_1)$ and $P_{Di} = f(z_i \geq 0 | \mathcal{H}_0)$.

Clearly, under the hypothesis $\mathcal{H}_0$ $(\mathcal{H}_1)$, u_i obeys the following distribution with the parameter of P_{fi} (P_{di}).

$$
P(u_i \,|\, \mathcal{H}_0) =
\begin{cases}
P_{fi} & u_i = +1 \\
1 - P_{fi} & u_i = -1
\end{cases}
$$

$$
P(u_i \,|\, \mathcal{H}_1) =
\begin{cases}
1 - P_{mi} & u_i = +1 \\
P_{mi} & u_i = -1
\end{cases}
$$

Then, under the hypothesis $\mathcal{H}_j$, the equivalent probability of false alarm and miss detection can be written as:

$$
\begin{aligned}
P_{Fi} = f(z_i \geq 0 \,|\, \mathcal{H}_0) &= \sum_{u_i \in \{+1, -1\}} f(z_i \geq 0 \,|\, u_i) P(u_i \,|\, \mathcal{H}_0) \\
&= f(z_i \geq 0 \,|\, u_i = +1) P_{fi} + f(z_i \geq 0 \,|\, u_i = -1)(1 - P_{fi})
\end{aligned}
\tag{22}
$$

$$
\begin{aligned}
P_{Di} = f(z_i \geq 0 \,|\, \mathcal{H}_1) &= \sum_{u_i \in \{+1, -1\}} f(z_i \geq 0 \,|\, u_i) P(u_i \,|\, \mathcal{H}_1) \\
&= f(z_i \geq 0 \,|\, u_i = +1) P_{di} + f(z_i \geq 0 \,|\, u_i = -1)(1 - P_{di})
\end{aligned}
\tag{23}
$$

Without loss of generality, suppose that the reporting channels between SVUs and FC is also Rayleigh fading channel draw from CSCG distribution $\mathcal{CN}(0, 2)$. In the other words, the PDF of the channel gain g_i can be represented as

$$
f(g_i) =
\begin{cases}
g_i \exp\left(-\frac{g_i^2}{2} \right) & g_i \geq 0 \\
0 & g_i < 0
\end{cases}
\tag{24}
$$

On the basis of the fact that $y_i = g_i u_i$, $z_i = y_i + w_i$ and w_i is a zero-mean Gaussian variable with variance δ_i^2, we can easily get

$$
f(y_i \,|\, u_i) =
\begin{cases}
u_i y_i \exp\left(-\frac{y_i^2}{2} \right) & y_i \geq 0 \\
0 & y_i < 0
\end{cases}
\tag{25}
$$

$$
f(z_i \,|\, y_i) = \frac{1}{\sqrt{2\pi}\delta_i} \exp\left(-\frac{(z_i - y_i)^2}{2\delta_i^2} \right)
\tag{26}
$$

Further still, according to this fact that $f(z_i | y_i, u_i) = f(z_i | y_i)$, which is stemmed from the fact that $(h_i, u_i) \to y_i \to z_i$ is a Markov chain, we can safely come to the following result

$$f(z_i | u_i) = \frac{f(z_i, u_i)}{p(u_i)} = \frac{\int f(z_i | y_i, u_i) f(y_i | u_i) p(u_i) dy_i}{p(u_i)}$$

$$= \int f(z_i | y_i) f(y_i | u_i) dy_i \tag{27}$$

Then, substituting (25) and (26) into (27), we can obtain the conditional PDF of the received observation z_i, given the local decision $u_i = +1$, as

$$f(z_i | u_i = +1) = \int_0^\infty \frac{1}{\sqrt{2\pi}\delta_i} \exp\left(-\frac{(z_i - y_i)^2}{2\delta_i^2}\right) y_i \exp\left(-\frac{y_i^2}{2}\right) dy_i$$

$$= \frac{1}{\sqrt{2\pi}\delta_i} \exp\left(-\frac{z_i^2}{2(1+\delta_i^2)}\right) \int_0^\infty y_i \exp\left(-\frac{(y_i - \frac{z_i}{1+\delta_i^2})^2}{\frac{2\delta_i^2}{1+\delta_i^2}}\right) dy_i \tag{28}$$

More specifically performing a change of variable $t = y_i - \frac{z_i}{1+\delta_i^2}$ and making the best of the integral properties of $\mathcal{Q}$-function, we can obtain

$$f(z_i | u_i = +1) = \frac{C^2 \delta_i^3}{\sqrt{2\pi}} \exp\left(-\frac{z_i^2}{2\delta_i^2}\right)\left[1 + \sqrt{2\pi}C z_i \exp\left(\frac{C^2 z_i^2}{2}\right)\mathcal{Q}(-C z_i)\right] \tag{29}$$

where $C = \frac{1}{\delta_i\sqrt{1+\delta_i^2}}$, $\mathcal{Q}(-x) = 1 - \mathcal{Q}(x)$.

Integrating both sides of (29) with respect to z_k, we can obtain

$$P(z_i \geq 0 | u_i = +1) = \int_0^\infty f(z_i | u_i = +1) dz_i$$

$$= \frac{C^2 \delta_i^3}{\sqrt{2\pi}} \int_0^\infty \left[\exp\left(-\frac{z_i^2}{2\delta_i^2}\right) + \frac{\sqrt{2\pi}}{\delta_i\sqrt{1+\delta_i^2}} z_i \exp\left(-\frac{z_i^2}{2(1+\delta_i^2)}\right)\mathcal{Q}\left(-\frac{z_i}{\delta_i\sqrt{1+\delta_i^2}}\right)\right] dz_i$$

$$= \frac{\delta_i}{\sqrt{2\pi}(1+\delta_i^2)}\left[\frac{\sqrt{2\pi}\delta_i}{2} + \frac{\sqrt{2\pi}\sqrt{1+\delta_i^2}}{2\delta_i} + \frac{\sqrt{2\pi}}{2\delta_i}\right]$$

$$= \frac{1}{2} + \frac{1}{2\sqrt{1+\delta_i^2}} = \frac{1}{2}\left(1 + \sqrt{\frac{\gamma_i}{2+\gamma_i}}\right) \tag{30}$$

where γ_i denotes the SNR of the Rayleigh fading reporting channel.

A similar analysis can be conducted for the case of $u_i = -1$, we have

$$f(z_i | u_i = -1) = \frac{C^2 \delta_i^3}{\sqrt{2\pi}} \exp\left(-\frac{z_i^2}{2\delta_i^2}\right)\left[1 - \sqrt{2\pi}C z_i \exp\left(\frac{C^2 z_i^2}{2}\right)\mathcal{Q}(C z_i)\right] \tag{31}$$

$$P(z_i \geq 0 | u_i = -1) = \int_0^\infty f(z_i | u_i = -1) dz_i = \frac{1}{2}\left(1 - \sqrt{\frac{\gamma_i}{2+\gamma_i}}\right) \tag{32}$$

By substituting (30) and (32) in (22) and (23), and after some simplified calculations, we can obtain the equivalent local probability of false alarm and detection as

$$P_{Fi} = P(z_i \geq 0 \,|\mathcal{H}_0\,) = \frac{1}{2} + \left(P_{fi} - \frac{1}{2}\right)\sqrt{\frac{\gamma_i}{2+\gamma_i}} \tag{33}$$

$$P_{Di} = P(z_i \geq 0 \,|\mathcal{H}_1\,) = \frac{1}{2} + \left(P_{di} - \frac{1}{2}\right)\sqrt{\frac{\gamma_i}{2+\gamma_i}} \tag{34}$$

and

$$P_{Mi} = 1 - P_{Di} = \frac{1}{2} + \left(P_{mi} - \frac{1}{2}\right)\sqrt{\frac{\gamma_i}{2+\gamma_i}} \tag{35}$$

From (33) and (34), we can see that, if $P_{di} > \frac{1}{2}$, then $P_{Di} < P_{di}$. Only when $P_{di} < \frac{1}{2}$, then $P_{Di} > P_{di}$. In other words, the equivalent probability of miss detection at the FC high above the local probability of miss detection at each SUV. In the same manner, when $P_{fi} > \frac{1}{2}$, $P_{Fi} < P_{fi}$. Only when $P_{fi} < \frac{1}{2}$, the channel error "increases" P_{Fi} to be higher than P_{fi}. Without doubt, this is achieved with an accompanied rise in the probability of miss detection.

Besides, we also see that, as the reporting channel becomes more unreliable (low SNR situation, i.e., SNR $\gamma_i \to -\infty$), the equivalent probability P_{Di} (P_{Fi}) is close to $\frac{1}{2}$. As SNR $\gamma_i \to \infty$, P_{Di} (P_{Fi}) comes near to P_{di} (P_{fi}), I would like to say this is a perfect reporting channel.

4.2. Global Probability of False Alarm and Miss Detection

Assuming that the reporting channels do not interfere with each other, and the delay is negligible. Once the fusion center decodes $\{z_i = g_i u_i + w_i; i = 1, 2, \cdots, N\}$ and gets $\{v_i; i = 1, 2, \cdots, N\}$, a global test statistic based on the counting rule is calculated linearly as follows:

$$\Lambda = \sum_{i=1}^{N} v_i \begin{cases} \geq T & \mathcal{H}_1 \\ < T & \mathcal{H}_0 \end{cases} \tag{36}$$

where T is the global decision threshold of counting rule, which can be in the form of $T = \alpha N$. This means that T or more SVUs decide hypothesis $\mathcal{H}_1$, then the global decision is $\mathcal{H}_1$

From the preceding analysis, we can see that v_i is a binary random variable which follows a Bernoulli distribution characterized by the associated P_{Fi} and P_{Di}. It is noteworthy that the pairs (P_{Fi}, P_{Di}) of different SVUs are not really the same because the pairs (P_{fi}, P_{di}) or γ_i are different. So $\{v_i, i = 1, 2, \cdots, N\}$ is a set of independent and non-identically distributed random variables. In consequence, their sum $\Lambda = \sum_{i=1}^{N} v_i$ will not approach the Binomial distribution any more. This makes the theoretical analysis and evaluation of $\overline{Q}_m$ more sophisticated since it is indeed arduous to obtain a closed-form expression for such a distribution. Therefore, instead of relying on the exact distribution of Λ, we exploit a large-sample gaussian approximation for the sum of independent but not identically distributed random variables, known as the Lindberg-Feller CLT [20].

Theorem 1. *Lindberg-Feller Central Limit Theorem (LF-CLT)*

Assume that $\{X_i, i = 1, 2, \cdots, N\}$ is a set of independently and non-identically distributed random variables with mean $\mathrm{E}[X_i] = \mu_i$ and variance $\mathrm{D}[X_i] = \delta_i^2$. Further, assume that the two following regularity conditions are satisfied

$$\mathrm{D}[X_i] > \beta_1 \tag{37}$$

and

$$\mathrm{E}\left[\,|X_i - \mathrm{E}[X_i]|^3\,\right] < \beta_2 \tag{38}$$

where β_1 and β_2 are positive values. Then, for sufficiently big N, $\sum_{i=1}^{N} X_i$ converges asymptotically to a Gaussian distribution characterized by

$$\sum_{i=1}^{N} X_i \to \mathcal{N}\left(\sum_{i=1}^{N} \mu_i,\ \sum_{i=1}^{N} \delta_i^2\right) \tag{39}$$

For the applicability of LF-CLT, we will show how above-mentioned Lindberg-Feller conditions are satisfied in the Appendix. Consequently, in a large cognitive vehicular network, the LF-CLT can be used to approximately describe the distribution of the global decision statistic under both hypothesis $\mathcal{H}_0$ and $\mathcal{H}_1$.

Because $\{v_i, i = 1, 2, \cdots, N\}$ are all independent of each other, when N is sufficient large, in light of the LF-CLT [20], Λ is asymptotically Gaussian distributed with mean

$$\mu = \mathrm{E}\{\Lambda\} = \sum_{i=1}^{N} \mathrm{E}\{v_i\} = \begin{cases} \sum_{i=1}^{N} P_{Fi} & \mathcal{H}_0 \\ \sum_{i=1}^{N} P_{Di} & \mathcal{H}_1 \end{cases} \tag{40}$$

and variance

$$\sigma^2 = \mathrm{D}\{\Lambda\} = \sum_{i=1}^{N} \mathrm{D}\{v_i\} = \begin{cases} \sum_{i=1}^{N} P_{Fi}(1 - P_{Fi}) & \mathcal{H}_0 \\ \sum_{i=1}^{N} P_{Di}(1 - P_{Di}) & \mathcal{H}_1 \end{cases} \tag{41}$$

Consequently, the global probability of false alarm and miss detection at the FC in this case can be described by

$$Q_f = \mathcal{Q}\left(\frac{T - \overline{\mu}}{\sqrt{\overline{\sigma^2}}}\right) = Q\left(\frac{T - \sum_{i=1}^{N} P_{Fi}}{\sqrt{\sum_{i=1}^{N} P_{Fi}\left(1 - P_{Fi}\right)}}\right) \tag{42}$$

$$Q_m = \mathcal{Q}\left(\frac{\overline{\mu} - T}{\sqrt{\overline{\sigma^2}}}\right) = \mathcal{Q}\left(\frac{\sum_{i=1}^{N} P_{Di} - T}{\sqrt{\sum_{i=1}^{N} P_{Di}\left(1 - P_{Di}\right)}}\right) \tag{43}$$

When the prior probabilities of presence and absence of PU are equal, i.e., $P(\mathcal{H}_1) = P(\mathcal{H}_0) = \frac{1}{2}$, the total probability of error detection can be written as

$$\begin{aligned} Q_e &= \mathcal{Q}_f + \mathcal{Q}_m \\ &= \mathcal{Q}\left(\frac{T - \sum_{i=1}^{N} P_{Fi}}{\sum_{i=1}^{N} P_{Fi}\left(1 - P_{Fi}\right)}\right) + \mathcal{Q}\left(\frac{\sum_{i=1}^{N} P_{Di} - T}{\sum_{i=1}^{N} P_{Di}\left(1 - P_{Di}\right)}\right) \end{aligned} \tag{44}$$

5. Numerical and Simulation Results

In this section, both theoretical and simulated results are provided to illustrate spectrum sensing performance in cognitive vehicular networks. The PU signal is assumed to enjoy unit power and be any kind of modulated signal with carrier frequency of 900Mhz and bandwidth of 6MHz. The sampling frequency in energy detector is equal to the bandwidth of PU signals, at the same time, the number of sampling observations during a sensing interval is $L = 50$. For all simulation cases, the average SNR is assumed to be the same for all SVUs, e.g., $\eta_0 = $ -8 dB and $\gamma_0 = 5.5$ dB. The performances with respect to the local (global) probability of miss detection is estimated to meet the constraint on the

230 local (global) probability of false alarm of P_f (Q_f) = 0.1. The number of realizations made to compute
231 the simulating probability of miss detection is 10000, which are set to guarantee the simulation results
232 can validate the theoretic analysis in the low probability region.

233   Firstly, we manifest the performance of spectrum sensing with energy detector in non-cooperative
234 cases, which is a key springboard of the study in cooperative cases. In Fig. 4, we provide the curves
235 of the local sensing performance based on energy detection as a function of Doppler shift $F_d T_s$. With
236 the carrier frequency and the sampling interval fixed, $F_d T_s$ value goes up as the vehicle velocity v.
237 It is illustrated that the probability of miss detection declines with the increase of vehicle velocity.
238 This reason is that high mobility gives us an opportunity to achieve more received signal information,
239 thereby enables SVUs to obtain higher sensing performance.

240   In Fig. 5, we present the average $\overline{P}_m$ curves as a function of the average SNR of sensing channels.
241 The capability of energy detector declines quickly with the reduce of the average received SNR from
242 10dB to -12dB. It can be seen that the simulating results are in accordance with the theoretical analysis
243 for both $\mathcal{M}_1$ and $\mathcal{M}_3$, justifying the validity of the analysis. The figure indicates that the expression
244 (17) and (11) (18) give the corresponding upper and lower bounds of the average $\overline{P}_m$ for spectrum
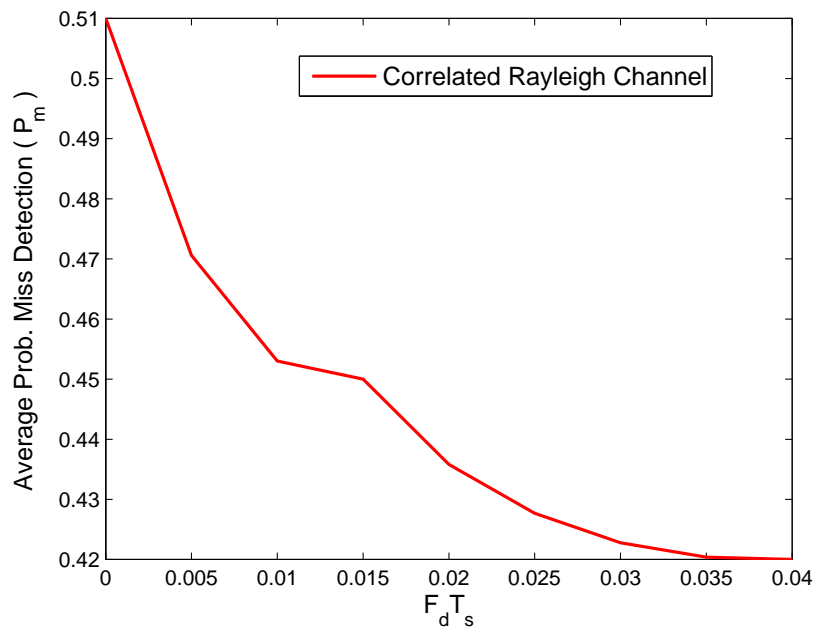245 sensing with energy detector under correlated Rayleigh fading channel.

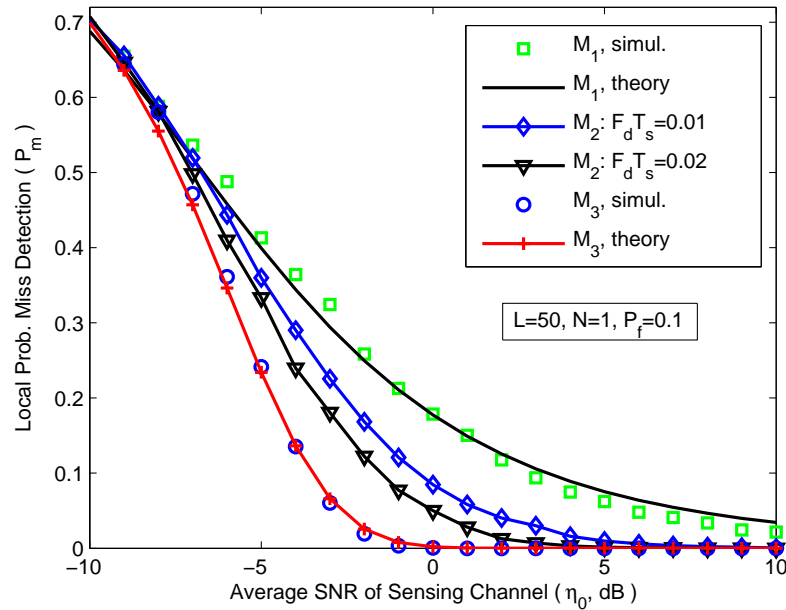**Figure 4.** The local probability of miss detection for various $F_d T_s$.

Figure 5. The local probability of miss detection for various average SNR of sensing channels.

Secondly, we focus on cooperative cases. In Fig. 6, we plot the global probability of miss detection (Q_m) as a function of the number of SUVs for hard fusion based on counting rule. As expected, the sensing performance shows an upward trend along with the increase of the number of SUVs. When N is extremely big, the global mis-detection probability approaches 0. For hard fusion, the Fig. 6 clearly demonstrate that the derived probability of miss detection based on Lindberg-Feller approximation is relatively poorer for a smaller number of SVUs. However, along with an increasing number of SVUs, the approximation asymptotically grows closer and closer to the exact sensing performance.

In Fig. 7, we present the ROC curves for different channel model. Note that, in the case of $\mathcal{M}_1$ and $\mathcal{M}_3$, we obtain the average mis-detection probability for local sensing, allowing for a much smoother global probability curve than the case of $\mathcal{M}_2$.

In Fig. 8, we present the average Q_m curves as a function of the average SNR of reporting channels. In the condition of poor reporting SNR, large bit error occurs, which severely degrade the detection performance. We can clearly see that cooperative sensing performance improves quickly with the increase of the average SNR of reporting channel from -8dB to 8dB. Note that the sensing performance in AWGN channel is always better than in Reyleigh channel.

In Fig. 9, we plot the global probability of error detection (Q_e) as a function of the local false-alarm probability. We can clearly see that, under certain conditions, there is an minimum probability of error detection, and that can be achieved when the local probabilities of false-alarm and mis-detection are equal ($P_f = P_m$). In Fig. 10, we plot the minimum achievable probability of error detection (Q_e) as a function of the number of SUVs.
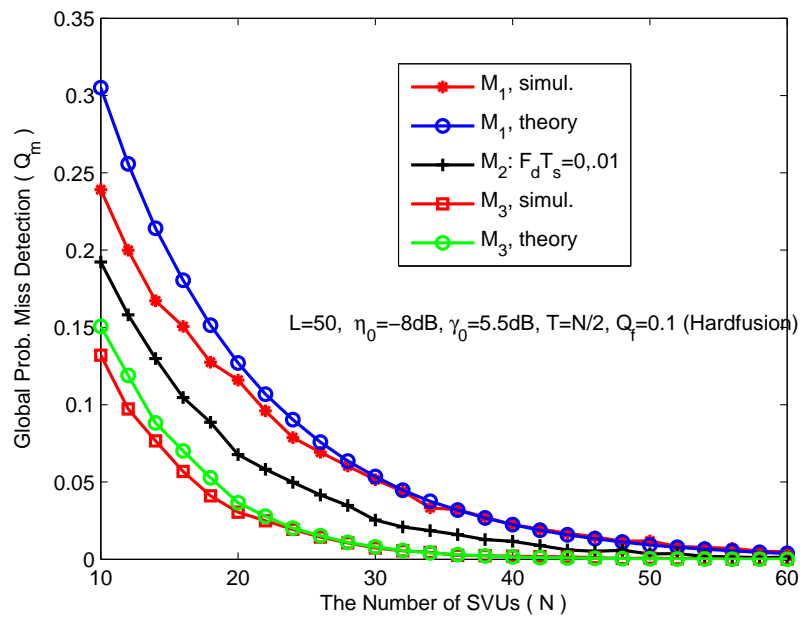
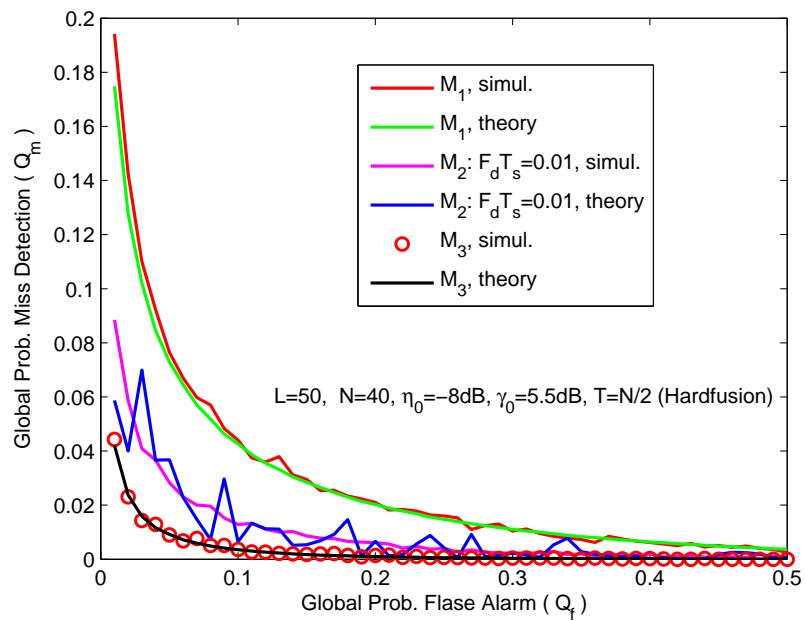**Figure 6.** The global probability of miss detection for various number of SUVs.

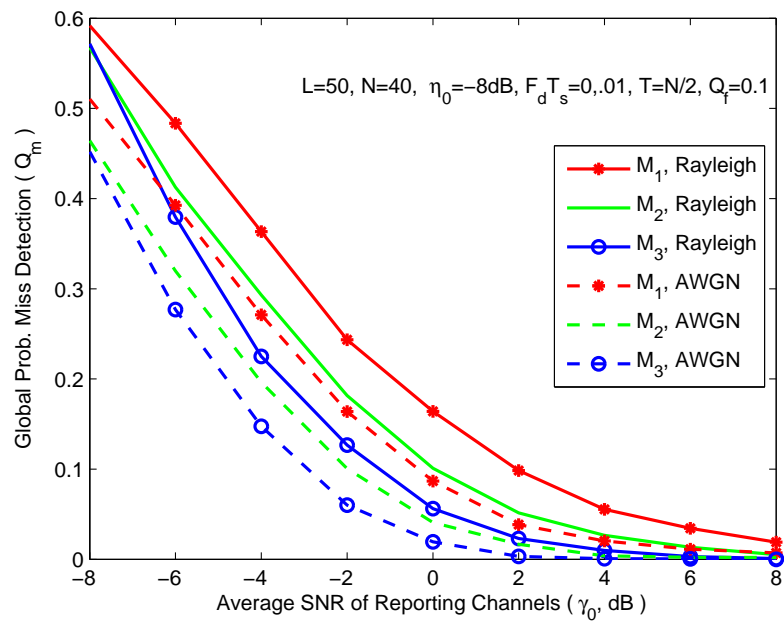**Figure 7.** ROC curves for different channel model.

Figure 8. The global probability of miss detection for various average SNR of reporting channels.
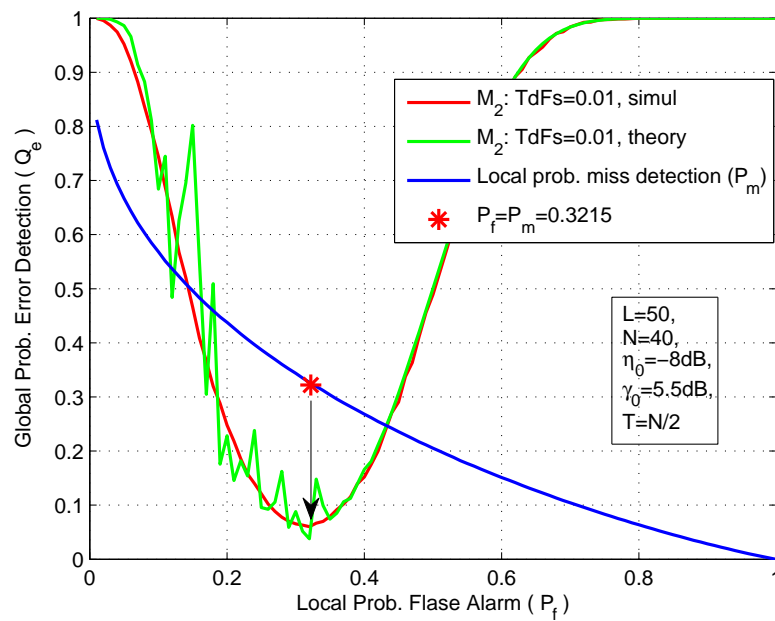

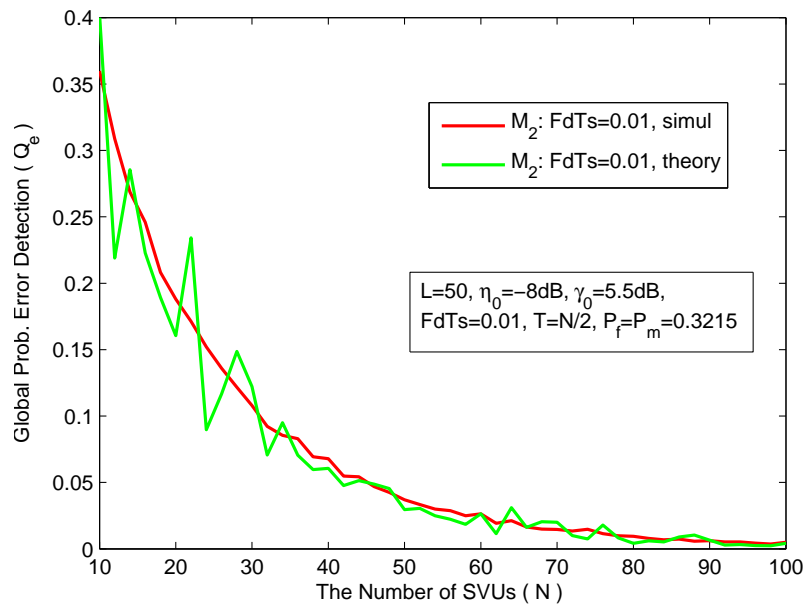**Figure 9.** The global probability of error detection for various local probability of flase alarm.

Figure 10. The global probability of error detection for various number of SVUs.

6. Conclusion

In this paper, we have researched the application of cognitive radio technique to vehicular environments for purpose of improving the reliability for vehicular communications. And for this, we evaluated the detection performance of spectrum sensing in mobile vehicular environments. Simulation results demonstrate that temporally correlation can not be neglected and be one of the considerable factors that may impact the sensing performance. In particular, highly mobility of the vehicles provides the opportunity to exploit temporal diversity at each vehicle. In spite of the fact that cooperative sensing have normally been considered as a viable means of producing better detection performance by making the most of spatial diversity among vehicles, we do believe that due to highly mobility, temporal diversity may be used in preference over vehicles' cooperation in the coming future.

Author Contributions: Xiaomin Qian designed the system model, performed performance evaluations by theoretical analysis and simulation, and prepared the manuscript. Li Hao conceived the system model, carried out theoretical analysis and supervised the activities. Dadong Ni and Quang Thanh Tran discussed the main ideas and analyzed the results together. All authors approved the publication.

Conflicts of Interest: The authors declare no conflict of interest.

Appendix

In the following, we make clear how the two sufficient conditions (37) and (38) for the LF-CLT are satisfied for $\Lambda = \sum_{i=1}^{N} v_i$ under hypothesis $\mathcal{H}_j$, for $j = 0, 1$. Notice that in the LF-CLT, essentially, the objective of the two conditions is to ensure that no single random variable is dominate in its contribution to the summation operator.

In the first step we shall prove that the first condition is satisfied. As can be seen from (21) and (34), the variance of v_i, for $k = 1, 2, \cdot, N$, under the hypotheses $\mathcal{H}_1$ can be represented as

$$
\begin{aligned}
D[v_i \,|\mathcal{H}_1] &= P_{Di} \left(1 - P_{Di} \right) \\
&= \left[\frac{1}{2} + \left(P_{di} - \frac{1}{2} \right) \sqrt{\frac{\gamma_i}{1 + \gamma_i}} \right] \left[\frac{1}{2} - \left(P_{di} - \frac{1}{2} \right) \sqrt{\frac{\gamma_i}{1 + \gamma_i}} \right] \\
&= \frac{1}{4} - \left(P_{di} - \frac{1}{2} \right)^2 \left(\frac{\gamma_i}{1 + \gamma_i} \right)
\end{aligned}
\tag{A1}
$$

It is sufficient to show that, under the hypothesis $\mathcal{H}_1$, the variance of v_i is lower bounded by a positive value, as long as the P_{di} are bounded away from 0 and 1.

In the next step, we show that the second condition (38) is satisfied. Let us make use of the fact that v_i is a binary random variable which follows a Bernoulli distribution characterized by the associated P_{Fi} and P_{Di}. It is plain enough that under the hypotheses $\mathcal{H}_1$

$$
\begin{aligned}
\mathrm{E}\left[|v_i - \mathrm{E}[v_i]|^3 \,|\mathcal{H}_1 \right] &= P_{Di} \left(1 - P_{Di} \right) \left(P_{Di}^2 + (1 - P_{Di})^2 \right) \\
&< P_{Di} \left(1 - P_{Di} \right)
\end{aligned}
\tag{A2}
$$

Accordingly, it is straightforward to see that $P_{Di}(1 - P_{Di})$ is upper bounded by a positive value.

In the above analysis, we prove that the two sufficient conditions (37) and (38) in the LF-CLT are satisfied under the assumption of hypothesis $\mathcal{H}_1$ explicitly, but the same proved method can be carried out to demonstrate the effectiveness under the hypothesis $\mathcal{H}_0$.

References

1. Mitola J.; Maguire, G. Q. Cognitive radio: Making software radios more personal. *IEEE Pers. Commun.* **1999**, *6*, 13-18.

2. Haykin, S. Cognitive radio: Brain-empowered wireless communications. *IEEE J. Sel. Areas Commun.* **2005**, *23*, 201-220.

3. Singh, K. D.; Rawat, P.; Bonnin, J. Cognitive radio for vehicular ad hoc networks (CR-VANETs): approaches and challenges. *EURASIP J. wireless commun. net.* **2014**, 2014.1: 49.

4. Wang, X. Y.; Ho, P. H. A Novel Sensing Coordination Framework for CR-VANETs. *IEEE Trans. Veh. Technol.* **2010**, *59*, 1936-1948.

5. Ali, A.; Hamouda, W. Advances on Spectrum Sensing for Cognitive Radio Networks: Theory and Applications. *IEEE Commun. surveys tut.* **2017**, *19*, 1277-1304.

6. Cicho-, K.; Kliks, A.; Bogucka, H. Energy-efficient cooperative spectrum sensing: A survey. *IEEE Commun. Surveys Tut.* **2016**, *18*, 1861-1886.

7. Mumtaz, S.; Huq, K. M. S.; Ashraf, M. I.; Rodriguez, J.; Monteiro, V.; Politis, C. Cognitive Vehicular Communication for 5G. IEEE Commun. Maga. **2015**, *53*, 109-117.

8. Felice, M. D.; Chowdhury, K. R.; Bononi, L. Analyzing the potential of cooperative Cognitive Radio technology on inter-vehicle communication. In Proceedings of the IFIP Wireless Days, Venice, Italy, 1-6, Oct. 2010.

9. Rasheed, H.; Rajatheva, N. Spectrum sensing for cognitive vehicular networks over composite fading. *Int. J. Veh. Technol.*, **2011**, *2011*, 1-9.

10. Liu, Y.; Xie, S.; Yu, R.; Zhang, Y.; Zhang, X.; Yuen, C. Exploiting temporal and spatial diversities for spectrum sensing and access in cognitive vehicular net- works. *Wireless Commun. Mobile Comput.* **2015**, *15*, 2079-2094.

11. Aygun, B.; Wyglinski, A. M. A Voting Based Distributed Cooperative Spectrum Sensing Strategy for Connected Vehicles. *IEEE Trans. Veh. Technol.*, **2017**, *66*, 5109-5121.

12. Chembe, C., Noor, R. M., Ahmedy, I., Oche, M., Kunda, D., Liu, C. H. "Spectrum sensing in cognitive vehicular network: State-of-Art, challenges and open issues," *Computer Commun.* **2017**, *97*, 15-30.

13. Rahaman, M. F.; Khan, M. Z. Low Complexity Optimal Hard Decision Fusion under Neyman-Pearson Criterion. *IEEE Signal Process. Lett.* **2017**, *1*, 1-5.

14. Chaudhari, S.; Lunden, J.; Koivunen, V.; Poor, H. V. Cooperative sensing with imperfect reporting channels: Hard decisions or soft decisions? *IEEE Trans. Signal Process.* **2012**, *60*, 18-28.

15. Simon, M. K.; Alouini, M. *Digital communication over fading channels.*, Vol. 95, John Wiley & Sons, 2005.

16. Tsitsiklis, J. N. Decentralized detection. *Advances in Statistical Signal Processing*. Greenwich, CT: JAI, **1993**, *2*, 297-344.

17. Herath, S. P.; Rajatheva, N.; Tellambura, C. Energy detection of unknown signals in fading and diversity reception. *IEEE Trans. Commun.*, **2011**, *59*, 2443-2453.

18. Atapattu, S.; Tellambura, C.; Jiang, H. Energy detection based cooperative spectrum sensing in cognitive radio networks. *IEEE Trans. wireless commun.*, **2011**, *10*, 1232-1241.

19. Nuttall, A. H. *Some integrals involving the Q-function.* DTIC Document, Tech.Rep., 1972.

20. Peebles, P. Z.; Shi, B. E. *Probability, random variables, and random signal principles.* McGraw-Hill: New York, USA, 2001.